Voltage Violation Prediction in Unobservable Distribution Systems

Mohammad Abujubbeh, *Student Member, IEEE*, Shweta Dahale, *Student Member, IEEE*, Balasubramaniam Natarajan, *Senior Member, IEEE*

***Abstract*—Recently, distributed energy resources (DERs) such as photovoltaic (PV) systems have garnered significant attention due to their economic and environmental benefits. However, DERs can also pose new technical challenges to distribution system operation including under/over voltage issues. In this regard, voltage violation prediction (VVP) becomes an essential component of system operation as it enables proactive control strategies. Unfortunately, classical voltage monitoring techniques assume full availability of state measurements across all nodes in the system. In real-world scenarios, distribution systems are limited with few measurement devices, rendering the system unobservable. Therefore, this paper proposes a new Bayesian matrix completion (BMC) based VVP technique that accurately predicts the probability of nodal voltage violations in unobservable (and unbalanced) distribution systems. The proposed approach is tested via simulations on the IEEE 37 test system. Results show that the proposed method offers over 90% violation prediction accuracy with as low as 50% fraction of available data.**

***Index Terms*—Distribution system, Distributed Energy Resources, Voltage Violation, State Estimation, Sensitivity Analysis**

I. Introduction

Distribution system operation has witnessed vast changes in the last decade due to exponential growth in energy demand and increased concerns about climate change, which motivated communities to invest in green DERs such as PV systems. Despite the benefits DERs offer to environment and consumers, e.g., reduced harmful emissions and lower energy prices, it has been shown that high level of DERs can impact nodal voltage stability in the system [1]. In this regard, utilities are interested in exploring efficient impact assessment tools that enable preemptive voltage violation prediction (VVP). This is mainly because preemptive monitoring tools significantly reduce the reliance on reactionary volt/var control strategies and enable more proactive schemes, in which optimal control signals can be implemented beforehand to prevent future violations. In this process, one of the major obstacles that stand in the face of optimal distribution system operation is system unobservability. In practical scenarios, state measurement devices are limited and exist at a small subset of nodes, rendering the system uobservable. Additional measurement devices can be installed to achieve system observability. Yet, this solution is not cost-effective and can be complex for large systems. Distribution system state estimation (DSSE) is an attractive alternative due to its cost effectiveness and estimation accuracy. Therefore, the development of efficient VVP that accounts for both complex power dynamics as well as system observability through DSSE is a vital step toward system modernization.

Early work on voltage monitoring involved learning from historical data, through which optimal system operation is implemented [2] [3]. More recent approaches in literature use traditional load flow based voltage sensitivity to derive a look-ahead prediction of nodal voltage states for predictive control purposes [1], [4], [5]. However, these methods do not account for uncertainty related to DER injections or load variability and their reliance on classical load flow based sensitivity makes them (1) computationally complex; and (2) non-scalable. Alternatively, authors in [6], [7] use Monte-Carlo based approaches to account for different DER sizes and derive the probability of nodal voltage violation. For example, [6] creates a large number of scenarios with different electric vehicle deployment capacities considering random spatial distribution. Similarly, [7] analyzes multiple scenarios to select the best load model for voltage regulation and loss minimization applications. It is important to note that such methods still do not consider temporal uncertainty of DERs or changeable load patterns but rather focus on analyzing the impact of multiple scenarios of DER capacities on voltage states, making them suitable only for planning applications. Few other methods focus on deep learning based prediction models for voltage violations such as deep neural network [8]. However, the hidden layers of such models makes it difficult to provide guarantee of performance against known or unknown errors in voltage states. Newer approaches introduce the paradigm of probabilistic voltage sensitivity analysis (PVSA) that is accurate and more computationally efficient when compared to classical load flow sensitivity [9]–[11]. However, these studies do not consider distribution system unobservability. Specifically, [9], [11] assume full knowledge of temporal voltage states (e.g., voltage current updates) to derive the probability distribution of predicted voltage states. However, this is not a realistic assumption since distribution systems are characterized with low-observability [12].

Therefore, the aim of this paper is to address this research gap via incorporating Bayesian matrix completion (BMC) based DSSE within the PVSA framework. The following summarizes the main contributions of the proposed approach:

- This paper proposes a novel probabilistic VVP mechanism in low-observable unbalanced distribution systems.

Mohammad Abujubbeh, Shweta Dahale, and Balasubramaniam Natarajan are with Electrical and Computer Engineering, Kansas State University, Manhattan, KS-66506, USA, (e-mail: abujubbeh@ksu.edu, sddahale@ksu.edu, bala@ksu.edu)

2022 IEEE Power & Energy Society General Meeting (PESGM) | 978-1-6654-0823-3/22/$31.00 ©2022 IEEE | DOI: 10.1109/PESGM48719.2022.9916805

978-1-6654-0823-3/22/$31.00 ©2022 IEEE
Authorized licensed use limited to: Kansas State University. Downloaded on June 26,2023 at 13:46:48 UTC from IEEE Xplore. Restrictions apply.

- The proposed approach that integrates DSSE and forecast based PVSA incorporates uncertainty of complex power changes due to PV injections and accounts for distribution system unobservability and measurement errors.
- The unique approach systematically exploits the uncertainties in system states while computing the VVP probabilities.
- The proposed approach provides 90% VVP accuracy with 50% fraction of available data, which makes it a suitable tool for predictive voltage control applications in modern distribution systems.

II. Proposed Approach

The proposed VVP technique is summarized in Fig. 1 and the functional blocks are detailed in this section. It is assumed that measurements come from SCADA system carrying information about active and reactive power as well as real and imaginary parts of nodal voltages. SCADA measurements are collected through sensor data aggregation system and sent for DSSE. It is important to mention that SCADA measurements are available only at a subset of nodes as highlighted by the bold circles in Fig. 1. To estimate the states at all nodes, BMC based DSSE is used and the corresponding estimation variance is derived. Finally, state estimates, their variance, and available measurements are used within the PVSA framework to derive the probability distribution of future nodal voltage states ($\mathbf{V}_O^f$) in real-time. This allows for the computation of probability of voltage violation induced by complex power fluctuations at any location in the system. It is assumed that complex power changes occur due to time-varying PV injections and variable load patterns.

A. BMC based system observability

DSSE task is difficult due to the lack of sufficient measurements making the system unobservable [13]. Consider an unbalanced distribution system with $\mathcal{N}$ nodes. Let $\mathbf{X}$ denote a matrix that contains information on nodal complex power values, real and imaginary parts of voltage, and voltage magnitudes for all nodes $\mathcal{N}$ in the system. In practice, due to limited number of measurements in the distribution system, only some elements of the matrix $\mathbf{X}$ are known (i.e., $\mathbf{X}$ is incomplete). BMC aims to complete this matrix $\mathbf{X}$ by estimating the unobserved states based on a suitable low rank approximation [14]. The low rank property in the matrix $\mathbf{X}$ results due to: (1) spatial correlation between measurements at different locations; and (2) the correlation between different types of measurements via power-flow equations. If we assume that the measurements at the slack bus are known, it is possible to use the measurements at the non-slack buses to construct the data matrix.

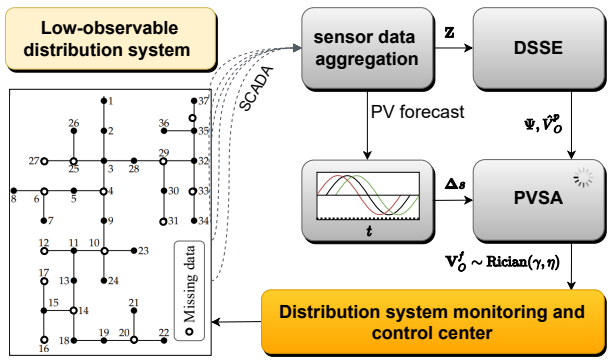

Fig. 1: VVP flowchart.

Let $m \in \mathcal{N}$ denote the set of phases at all the non-slack buses. The measurement matrix $\mathbf{Z}$ is constructed such that each row represents a phase and each column represents the measurement associated with the phase of each bus. For each $b \in m$, each row of the matrix $\mathbf{Z} \in \mathbb{R}^{m \times n}$ with $n = 5$ is structured as,

$$[\mathbf{P}_b, \mathbf{Q}_b, \Re(\mathbf{v}_b), \Im(\mathbf{v}_b), |\mathbf{v}_b|], \tag{1}$$

where, $\mathbf{P}_b$ and $\mathbf{Q}_b$ represent the active power and reactive power injections at each phase of non-slack bus b respectively. The terms $\Re(\mathbf{v}_b)$ and $\Im(\mathbf{v}_b)$ represent the real and imaginary parts of voltage phasors at each phase of non-slack buses, respectively. Let $\Omega \subseteq \{1, ..., m\} \times \{1, ..., n\}$ describe the known entries in $\mathbf{Z}$. The known entries can also be written as,

$$\mathbf{Z}_{lj} = \mathbf{X}_{lj} + \mathbf{N}_{lj}, \quad (l, j) \in \Omega \tag{2}$$

where, $\mathbf{X}_{lj}$ and $\mathbf{N}_{lj}$ refers to the row entry l and column entry j in the matrix $\mathbf{X}$ and $\mathbf{N}$, respectively. The unknown low rank matrix $\mathbf{X}$ is factorized into two matrices as $\mathbf{X} = \mathbf{A}\mathbf{B}^\intercal$. Here, $\mathbf{A}$ is an $m \times r$ matrix and $\mathbf{B}$ is an $n \times r$ matrix such that rank($\mathbf{X}$) = r. The matrix $\mathbf{X}$ is the sum of the outer-products of the columns of $\mathbf{A}$ and $\mathbf{B}$ such that,

$$\mathbf{X} = \sum_{l=1}^{k} \mathbf{a}_{.l} \mathbf{b}_{.l}^\intercal \tag{3}$$

where, $k \geq r$, $\mathbf{a}_{.l}$ and $\mathbf{b}_{.l}$ denote the l^{th} column of matrix $\mathbf{A}$ and $\mathbf{B}$ respectively. The l^{th} row of matrix $\mathbf{A}$ and $\mathbf{B}$ is represented by $\mathbf{a}_{l.}$ and $\mathbf{b}_{l.}$ respectively. The low rank matrix is obtained by setting most of the columns in $\mathbf{A}$ and $\mathbf{B}$ to zero. To achieve this condition, the columns of $\mathbf{A}$ and $\mathbf{B}$ are associated with Gaussian priors of precisions γ_l, that is

$$\mathbf{p}(\mathbf{A}|\boldsymbol{\gamma}) = \prod_{l=1}^{k} \mathcal{N}(\mathbf{a}_{.l}|\mathbf{0}, \gamma_l^{-1}\mathbf{I}_m) \tag{4}$$

$$\mathbf{p}(\mathbf{B}|\boldsymbol{\gamma}) = \prod_{l=1}^{k} \mathcal{N}(\mathbf{b}_{.l}|\mathbf{0}, \gamma_l^{-1}\mathbf{I}_n) \tag{5}$$

During inference, most of the γ_l's take large values, thus forcing the columns of $\mathbf{A}$ and $\mathbf{B}$ to go to zero. The columns of $\mathbf{A}$ and $\mathbf{B}$ have the same sparsity profile enforced by the common precisions γ_l. These sparsity priors on the factorized matrix encourages low-rank solutions. The precision γ_l are assumed to have a Gamma hyperprior given as,

$$\mathbf{p}(\gamma_l) = Gamma(c, \frac{1}{d}) \tag{6}$$

978-1-6654-0823-3/22/$31.00 ©2022 IEEE
Authorized licensed use limited to: Kansas State University. Downloaded on June 26,2023 at 13:46:48 UTC from IEEE Xplore. Restrictions apply.

The parameters c and d are set to small values to obtain broad hyperpriors. Using the model (2) and factorized matrices $\mathbf{A}$ and $\mathbf{B}$, the conditional distribution of the observations are obtained as,

$$\mathbf{p}(\mathbf{Z}|\mathbf{A},\mathbf{B}) = \prod_{(l,j)\in\Omega} \mathcal{N}(Z_{lj}|X_{lj},\beta^{-1}) \tag{7}$$

where β is the noise precision of each measurement. The joint distribution is therefore given as,

$$\mathbf{p}(\mathbf{Z},\mathbf{A},\mathbf{B},\boldsymbol{\gamma}) = \mathbf{p}(\mathbf{Z}|\mathbf{A},\mathbf{B})\mathbf{p}(\mathbf{A}|\boldsymbol{\gamma})\mathbf{p}(\mathbf{B}|\boldsymbol{\gamma})\mathbf{p}(\boldsymbol{\gamma}) \tag{8}$$

The evaluation of posterior distributions is obtained by mean field variational Bayes [14]. The posterior distribution of $\mathbf{A}$ and $\mathbf{B}$ decompose as independent distributions of their rows. The approximate posterior distributions of the latent variables are updated as,

$$\mathbf{q}(\mathbf{a}_{l\cdot}) = \mathcal{N}\left(\mathbf{a}_{l\cdot}|\langle\mathbf{a}_{l\cdot}\rangle, \boldsymbol{\Sigma}_l^a\right) \tag{9}$$

where the mean and covariance are defined as,

$$\langle\mathbf{a}_{l\cdot}\rangle^\intercal = \langle\beta\rangle\, \boldsymbol{\Sigma}_l^a \langle\mathbf{B}_l\rangle^\intercal \mathbf{z}_{l\cdot}^\intercal \tag{10}$$

$$\boldsymbol{\Sigma}_l^a = \left(\langle\beta\rangle \langle\mathbf{B}_l^\intercal\mathbf{B}_l\rangle + \boldsymbol{\Gamma}\right)^{-1} \tag{11}$$

Here,

$$\langle\mathbf{B}_l^\intercal\mathbf{B}_l\rangle = \sum_{j:(l,j)\in\Omega} \left(\langle\mathbf{b}_{j\cdot}^\intercal\rangle\langle\mathbf{b}_{j\cdot}\rangle + \boldsymbol{\Sigma}_j^b\right) \tag{12}$$

and $\boldsymbol{\Gamma} = diag(\boldsymbol{\gamma})$. Similarly, the posterior density of j^{th} row of $\mathbf{B}$ is found as,

$$\mathbf{q}(\mathbf{b}_{j\cdot}) = \mathcal{N}\left(\mathbf{b}_{j\cdot}|\langle\mathbf{b}_{j\cdot}\rangle, \boldsymbol{\Sigma}_j^b\right) \tag{13}$$

where the mean and covariance are defined as,

$$\langle\mathbf{b}_{j\cdot}\rangle^\intercal = \langle\beta\rangle\, \boldsymbol{\Sigma}_j^b \langle\mathbf{A}_j\rangle^\intercal \mathbf{z}_{\cdot j}^\intercal \tag{14}$$

$$\boldsymbol{\Sigma}_j^b = \left(\langle\beta\rangle \left\langle\mathbf{A}_j^\intercal\mathbf{A}_j\right\rangle + \boldsymbol{\Gamma}\right)^{-1} \tag{15}$$

The posterior density of γ_l becomes a gamma distribution

$$\mathbf{q}(\gamma_l) \propto \gamma_l^{\left(c-1+\frac{m+n}{2}\right)} \exp\left(-\gamma_l \frac{2d + \langle\mathbf{a}_{l\cdot}^\intercal\mathbf{a}_{l\cdot}\rangle + \langle\mathbf{b}_{l\cdot}^\intercal\mathbf{b}_{l\cdot}\rangle}{2}\right) \tag{16}$$

with mean,

$$\langle\gamma_l\rangle = \frac{2c+m+n}{2d + \langle\mathbf{a}_{l\cdot}^\intercal\mathbf{a}_{l\cdot}\rangle + \langle\mathbf{b}_{l\cdot}^\intercal\mathbf{b}_{l\cdot}\rangle} \tag{17}$$

The required expectations are given by

$$\langle\mathbf{a}_{l\cdot}^\intercal\mathbf{a}_{l\cdot}\rangle = \langle\mathbf{a}_{l\cdot}\rangle^\intercal\langle\mathbf{a}_{l\cdot}\rangle + \sum_j \left(\boldsymbol{\Sigma}_l^a\right)_{ll}, \tag{18}$$

$$\langle\mathbf{b}_{l\cdot}^\intercal\mathbf{b}_{l\cdot}\rangle = \langle\mathbf{b}_{l\cdot}\rangle^\intercal\langle\mathbf{b}_{l\cdot}\rangle + \sum_j \left(\boldsymbol{\Sigma}_l^b\right)_{ll} \tag{19}$$

The approximate posterior distribution of β is given as,

$$\langle\beta\rangle = \frac{(FAD)\times m\times n}{\langle\|\mathbf{Z} - P_\Omega(\mathbf{A}\mathbf{B}^\intercal)\|\rangle_F^2} \tag{20}$$

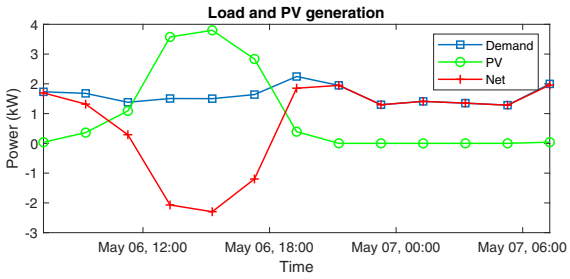

Fig. 2: PV generation and load profile.

The variance of estimated elements in the complete matrix $\mathbf{X}$ is given as,

$$\boldsymbol{\Psi}_{l,j} = tr(\mathbf{b}_{j\cdot}\boldsymbol{\Sigma}_l^a\mathbf{b}_{j\cdot}^\intercal) + tr(\mathbf{a}_{l\cdot}\boldsymbol{\Sigma}_j^b\mathbf{a}_{l\cdot}^\intercal) + tr(\boldsymbol{\Sigma}_j^b\boldsymbol{\Sigma}_l^a) \tag{21}$$

where, $tr(\cdot)$ is the trace. The next subsection describes VVP in low-observable distribution systems. Specifically, the estimated complete matrix $\mathbf{X}$ as well as the variance of estimates computed in $\boldsymbol{\Psi}$ will be used in a probabilistic sensitivity analysis framework for VVP.

B. Sensitivity based violation prediction

Voltage can fluctuate at any node (*observation node* O) in the system due to complex power changes at another node (*actor node* A). Nodal voltages may exceed safe operational limits (i.e., $0.95 < |V| < 1.05$ p.u) due to abrupt complex power changes at actor nodes, which is undesired for distribution system operation. Recent research [11] has shown that it is possible to predict such nodal voltage violations using PVSA. That is, if complex power at a particular actor node A changes from S_A to $S_A + \Delta S_A$, the voltage changes at any observation node O from V_O to $V_O + \Delta V_O$. In this process, the change in voltage ΔV_O can be linearly approximated with a tight upper bound that guarantees accuracy [10]. This approximation can then used to systematically incorporate uncertainty associated with complex power changes at actor nodes, which results in a unique probability distribution of the predicted voltage magnitude at observation nodes [11]. However, in actual distribution systems, voltage state measurements are not available at every node. Therefore, Theorem 1 provides the probability distribution of predicted voltage magnitude at observation nodes in low-observable distribution systems.

Theorem 1. *For a given unbalanced distribution system, the predicted voltage magnitude ($|V_O^f|$) at an observation node O due to complex power changes at multiple actor nodes $A \in \mathcal{A}$ in low-observable distribution systems follows a Rician distribution, i.e.,*

$$|V_O^f| \sim \textit{Rician}(\upsilon, \eta) \tag{22}$$

where, $\upsilon = \sqrt{\tau}$ and $\eta = \sqrt{\xi}$ with,

$$\xi = \frac{\sigma_r^4(1+2\mu_r^2) + \sigma_i^4(1+2\mu_i^2)}{\sigma_r^2(1+2\mu_r^2) + \sigma_i^2(1+2\mu_i^2)} \tag{23}$$

978-1-6654-0823-3/22/$31.00 ©2022 IEEE
Authorized licensed use limited to: Kansas State University. Downloaded on June 26,2023 at 13:46:48 UTC from IEEE Xplore. Restrictions apply.

and,

$$\tau = \frac{(\sigma_r^2\mu_r^2 + \sigma_i^2\mu_i^2)(\sigma_r^2 + \sigma_i^2 + 2\sigma_r^2\mu_r^2 + 2\sigma_i^2\mu_i^2)}{\sigma_r^4 + \sigma_i^4 + 2\sigma_r^4\mu_r^2 + 2\sigma_r^4\mu_i^2}. \quad (24)$$

Here, $\sigma_r^2 = \mathbf{\Psi}_{O,3} + \mathbf{c_r}^\intercal \mathbf{\Sigma_{\Delta S}} \mathbf{c_r}$, $\sigma_i^2 = \mathbf{\Psi}_{O,4} + \mathbf{c_i}^\intercal \mathbf{\Sigma_{\Delta S}} \mathbf{c_i}$, $\mu_r = \mathbf{X}_{O,3} + \mathbf{c_r^T} \boldsymbol{\mu}_{\boldsymbol{\Delta S}}$, *and* $\mu_i = \mathbf{X}_{O,4} + \mathbf{c_i^T} \boldsymbol{\mu}_{\boldsymbol{\Delta S}}$. $\mathbf{\Psi}_{O,3}$ *and* $\mathbf{\Psi}_{O,4}$ *represent the variance of real and imaginary parts of voltage estimates according to (21) whereas* $\mathbf{X}_{O,3}$ *and* $\mathbf{X}_{O,4}$ *are the present estimates of real and imaginary parts of voltage (3), respectively.* $\mathbf{c_r}$ *and* $\mathbf{c_i}$ *are based on system topology.* $\boldsymbol{\mu}_{\boldsymbol{\Delta S}}$ *is the mean of change in voltage states with* $\boldsymbol{\Delta S} = [\Delta P_1^a, ..., \Delta P_n^a, \Delta Q_1^a, ..., \Delta Q_n^a]^\intercal$ *is the vector of complex power changes and* $\mathbf{\Sigma_{\Delta S}}$ *is a the covariance matrix that contains the variance and cross-covariance terms of complex power change across different actor nodes as shown in Eq. (12) of [11].*

Proof. Let $\hat{\mathbf{V}}_\mathbf{O}^\mathbf{p}$ be the present voltage state at observation node O. It is possible to write the predicted future voltage state $\mathbf{V}_O^f$ in terms of the voltage change introduced by the DERs at actor nodes, i.e.,

$$\mathbf{V_O^f} = \hat{\mathbf{V}}_\mathbf{O}^\mathbf{p} + \mathbf{\Delta V_O}, \quad (25)$$

where $\mathbf{\Delta V_O}$ is the change in voltage states at observation nodes that is caused by complex power changes at DERs. More details on how to compute this voltage change can be found in [10]. To account for system unobservability, we use the real and imaginary parts of voltage estimates $\mathbf{X}_{O,3}$ and $\mathbf{X}_{O,4}$ as well as their estimation variance, i.e., $\mathbf{\Psi}_{O,3}$ and $\mathbf{\Psi}_{O,4}$, respectively. Therefore, the present voltage estimates $\hat{\mathbf{V}}_O^p$ can be written as,

$$\hat{\mathbf{V}}_\mathbf{O}^\mathbf{p} = [\hat{V}_O^{r,p}, \hat{V}_O^{i,p}]^\intercal \triangleq [\mathbf{X}_{O,3}, \mathbf{X}_{O,4}]^\intercal. \quad (26)$$

Follows from (20), the distribution of present voltage states follows a Gaussian distribution,

$$\hat{\mathbf{V}}_\mathbf{O}^\mathbf{p} \sim \mathcal{N}(\boldsymbol{\mu}_p, \mathbf{\Sigma}_p), \text{ with } \boldsymbol{\mu}_p = [\mathbf{X}_{O,3}, \mathbf{X}_{O,4}]^\intercal \quad (27)$$

and

$$\mathbf{\Sigma}_p = \begin{bmatrix} \mathbf{\Psi}_{O,3} & cov(\mathbf{X}_{O,3}, \mathbf{X}_{O,4}) \\ cov(\mathbf{X}_{O,4}, \mathbf{X}_{O,3}) & \mathbf{\Psi}_{O,4} \end{bmatrix} \forall O \in m \quad (28)$$

The distribution of $\mathbf{V_O^f}$ is based on the present voltage. Thus, the real and imaginary parts of $\mathbf{V_O^f} \triangleq [V_O^{r,f},\ V_O^{i,f}]^\intercal$ can be rewritten as $\mathbf{V_O^f} = [\mathbf{X}_{O,3},\ \mathbf{X}_{O,4}]^\intercal + [\Delta V_O^r,\ \Delta V_O^i]^\intercal$. Thus,

$$\mathbf{V_O^f} \sim \mathcal{N}\left(\begin{bmatrix} \mathbf{X}_{O,3} \\ \mathbf{X}_{O,4} \end{bmatrix} + \begin{bmatrix} \mathbf{c}_r^\intercal \boldsymbol{\mu}_{\boldsymbol{\Delta S}} \\ \mathbf{c}_i^\intercal \boldsymbol{\mu}_{\boldsymbol{\Delta S}} \end{bmatrix}, \begin{bmatrix} \lambda_r & \delta_f \\ \delta_f & \lambda_i \end{bmatrix} \right) \quad (29)$$

where, $\lambda_r = \mathbf{\Psi}_{O,3} + \mathbf{c}_r^\intercal \mathbf{\Sigma_{\Delta S}} \mathbf{c}_r$, $\lambda_i = \mathbf{\Psi}_{O,4} + \mathbf{c}_i^\intercal \mathbf{\Sigma_{\Delta S}} \mathbf{c}_i$, $\delta_f = cov(\mathbf{X}_{O,3}, \mathbf{X}_{O,4}) + \mathbf{c}_r^\intercal \mathbf{\Sigma_{\Delta S}} \mathbf{c}_i$. The terms $\mathbf{c}^\intercal \boldsymbol{\mu}_{\boldsymbol{\Delta S}}$ and $\mathbf{c}^\intercal \mathbf{\Sigma_{\Delta S}} \mathbf{c}$ are the mean and variance of real and imaginary voltage change caused by complex power changes at all actor nodes denoted by the subscripts r or i, respectively. The distribution of $|V_O^f|^2 = (V_O^{r,f})^2 + (V_O^{r,f})^2$ follows a scaled non-central chi-square with weight ξ, non-centrality parameter τ and $\rho = 1$ degrees of freedom as [11],

$$|V_O^f|^2 \sim \xi \chi_\rho^2(\tau) \quad (30)$$

where, ξ and τ are given in (23) and (24), respectively. $\sigma_r^2 = \mathbf{\Psi}_{O,3} + \mathbf{c}_r^\intercal \mathbf{\Sigma_{\Delta S}} \mathbf{c}_r$, $\sigma_i^2 = \mathbf{\Psi}_{O,4} + \mathbf{c}_i^\intercal \mathbf{\Sigma_{\Delta S}} \mathbf{c}_i$, $\mu_r = \mathbf{X}_{O,3} + \mathbf{c}_r^\intercal \boldsymbol{\mu}_{\boldsymbol{\Delta S}}$ and $\mu_r = \mathbf{X}_{O,4} + \mathbf{c}_i^\intercal \boldsymbol{\mu}_{\boldsymbol{\Delta S}}$. Since the square root of non-central chi-square random variables follows a Rician distribution, the magnitude of predicted voltage change will follow a Rician distribution,

$$|V_O^f| \sim \text{Rician}(\upsilon, \eta) \quad (31)$$

where, $\upsilon = \sqrt{\tau}$ and $\eta = \sqrt{\xi}$. □

III. Simulation results

This section validates the proposed VVP rule in low observable distribution systems. The method is verified on the unbalanced 37 node test system [15]. It is assumed that the system is unobservable with 50% as a fraction of available data as highlighted by the dark circles in Fig. 1. It is important to note that the proposed method is generic for any choice of nodes with missing data since the system is considered unobservable at 50% fraction of available data [12]. 14 actor nodes ($\mathcal{A} = [5, ..., 18]$) are randomly selected and integrated with PV units at phase a. PV active power injection is modeled as a random process with uncertainty component as,

$$\Delta P_{pv} = S(t) + r(t) \quad (32)$$

where, $S(t)$ is the mean forecast trend of PV active power injection and $r(t) \sim \mathcal{N}(0, \sigma_{pv}^2)$ is a zero mean Gaussian that incorporates injection variability with variance σ_{pv}^2. It is important to note that PVSA approach is also applicable where $r(t)$ is non-Gaussian [10]. Fig. 2 shows $S(t)$ as well as the load pattern of one actor node. The VVP is computed based on Theorem 1 over the entire time period and $\mathbf{V_O^p}$ for all nodes where state measurements are unavailable is estimated using BMC. Two scenarios are analyzed to show the effectiveness of the proposed method. For the first scenario, it is assumed that the state estimates ($[\mathbf{X}_{O,3}, \mathbf{X}_{O,4}]^\intercal$) are perfect, i.e., no process noise is injected in (27). The resulting violation prediction for this scenario is plotted in Fig. 3. This figure shows VVP using Theorem 1 compared to actual violation count computed by classical load flow method (simulation). It can be seen that using state estimates of the BMC, the prediction rule is accurate in preemptively identifying nodal voltage violations. Next, we assume that the knowledge of present voltage states at observation nodes ($\mathbf{V_O^p}$) is erroneous with covariance structure (28) based on the matrix $\mathbf{\Psi}$ in (21). Figures 4 and 5 show the mean and variance of real and imaginary parts of present voltage estimates. It can be seen that the variance of nodes where measurements are unavailable is higher than that of nodes where measurements are available. This variance is used together with errors in state measurements to validate the accuracy of the proposed approach. For validation, the simulation setup is repeated for 50 Monte Carlo simulations over different values of measurement errors and the prediction error is computed based on the different between the proposed approach and classical load flow method. It can be seen from Fig. 6 that it is possible to obtain low prediction errors as measurement error increases. For typical real world values

978-1-6654-0823-3/22/$31.00 ©2022 IEEE
Authorized licensed use limited to: Kansas State University. Downloaded on June 26,2023 at 13:46:48 UTC from IEEE Xplore. Restrictions apply.

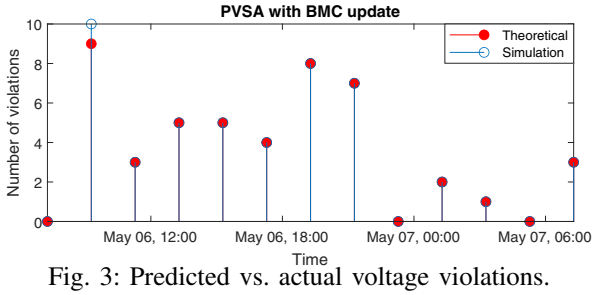

Fig. 3: Predicted vs. actual voltage violations.

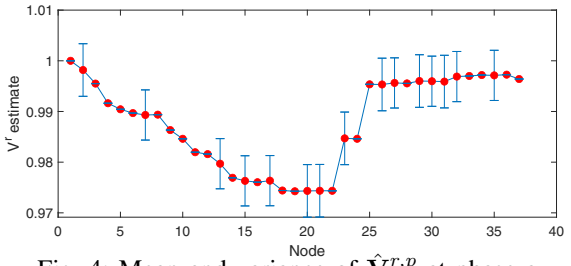

Fig. 4: Mean and variance of $\hat{\mathbf{V}}_O^{r,p}$ at phase a.

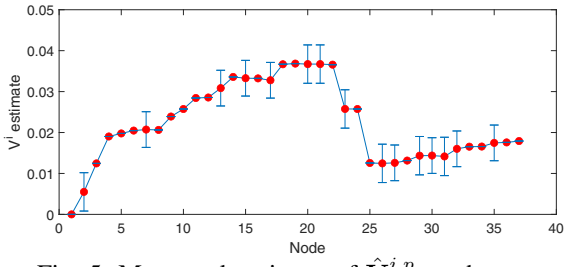

Fig. 5: Mean and variance of $\hat{\mathbf{V}}_O^{i,p}$ at phase a.

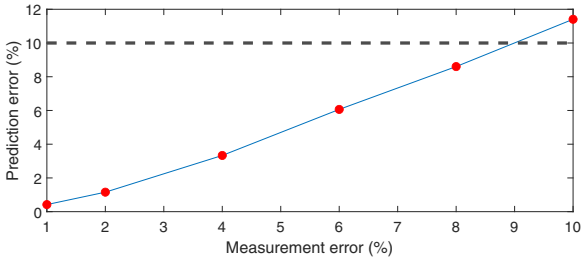

Fig. 6: Prediction accuracy with erroneous voltage states.

of measurement errors (e.g., at most 5-6% of actual values), the prediction accuracy is over 90%. This demonstrates the effectiveness of the proposed method against errors in the knowledge of present voltage states, which makes it suitable for proactive control applications.

IV. Conclusion

This paper presents an efficient VVP technique that is based on probabilistic sensitivity of nodal voltages to dynamic PV injections and variable load patterns. The proposed method incorporates system unobservability where SCADA measurements are limited to a subset of nodes in the system. For this BMC provides accurate estimates of present voltage states as well as their estimation variance. It has been shown through simulation that the proposed technique is accurate in predicting voltage violations when compared to actual load flow solution with as low as 50% fraction of available state measurements. In addition, the prediction error is found to be over 90% for different ranges of variance in measurement errors. This clearly shows that the proposed method is efficient and can be used for operational monitoring applications in modern distribution systems. Future research will focus on developing optimal proactive voltage control strategies using dominant influencer nodes of voltage fluctuations.

V. Acknowledgement

This material is based upon work partly supported by the Department of Energy, Office of Energy Efficiency and Renewable Energy (EERE), Solar Energy Technologies Office, under Award # DE-EE0008767 and National Science Foundation under award # 1855216.

References

[1] Q. Yang, G. Wang, A. Sadeghi, G. B. Giannakis, and J. Sun, "Two-timescale voltage control in distribution grids using deep reinforcement learning," *IEEE Transactions on Smart Grid*, vol. 11, no. 3, pp. 2313–2323, 2019.

[2] A. Kulmala, S. Repo, and P. Järventausta, "Coordinated voltage control in distribution networks including several distributed energy resources," *IEEE Transactions on Smart Grid*, vol. 5, no. 4, pp. 2010–2020, 2014.

[3] R. Tonkoski, L. A. Lopes, and T. H. El-Fouly, "Coordinated active power curtailment of grid connected pv inverters for overvoltage prevention," *IEEE Transactions on sustainable energy*, vol. 2, no. 2, pp. 139–147, 2010.

[4] A. Cagnano and E. De Tuglie, "Centralized voltage control for distribution networks with embedded pv systems," *Renewable Energy*, vol. 76, pp. 173–185, 2015.

[5] H. J. Liu, W. Shi, and H. Zhu, "Hybrid voltage control in distribution networks under limited communication rates," *IEEE Transactions on Smart Grid*, vol. 10, no. 3, pp. 2416–2427, 2018.

[6] P. Papadopoulos, S. Skarvelis-Kazakos, I. Grau, L. M. Cipcigan, and N. Jenkins, "Predicting electric vehicle impacts on residential distribution networks with distributed generation," in *2010 IEEE Vehicle Power and Propulsion Conference*. IEEE, 2010, pp. 1–5.

[7] D. Singh, R. K. Misra, and D. Singh, "Effect of load models in distributed generation planning," *IEEE Transactions on Power Systems*, vol. 22, no. 4, pp. 2204–2212, 2007.

[8] M. Mokhtar, V. Robu, D. Flynn, C. Higgins, J. Whyte, C. Loughran, and F. Fulton, "Predicting the voltage distribution for low voltage networks using deep learning," in *2019 IEEE PES Innovative Smart Grid Technologies Europe (ISGT-Europe)*. IEEE, 2019, pp. 1–5.

[9] K. Jhala, V. Krishnan, B. Natarajan, and Y. Zhang, "Data-driven preemptive voltage monitoring and control using probabilistic voltage sensitivities," in *2019 IEEE Power & Energy Society General Meeting (PESGM)*. IEEE, 2019, pp. 1–5.

[10] S. Munikoti, B. Natarajan, K. Jhala, and K. Lai, "Probabilistic voltage sensitivity analysis to quantify impact of high pv penetration on unbalanced distribution system," *IEEE Transactions on Power Systems*, 2021.

[11] M. Abujubbeh, S. Munikoti, and B. Natarajan, "Probabilistic voltage sensitivity based preemptive voltage monitoring in unbalanced distribution networks," *arXiv preprint arXiv:2008.10814*, 2020.

[12] S. Dahale, H. S. Karimi, K. Lai, and B. Natarajan, "Sparsity based approaches for distribution grid state estimation - a comparative study," *IEEE Access*, vol. 8, pp. 198 317–198 327, 2020.

[13] S. Dahale and B. Natarajan, "Joint matrix completion and compressed sensing for state estimation in low-observable distribution system," in *2021 IEEE PES Innovative Smart Grid Technologies Conference - Latin America (ISGT Latin America)*, 2021, pp. 1–5.

[14] S. D. Babacan, M. Luessi, R. Molina, and A. K. Katsaggelos, "Sparse bayesian methods for low-rank matrix estimation," *IEEE Transactions on Signal Processing*, vol. 60, no. 8, pp. 3964–3977, 2012.

[15] "IEEE PES AMPS DSAS Test Feeder Working Group," https://site.ieee.org/pes-testfeeders/resources/, accessed: 2021-08-10.

978-1-6654-0823-3/22/$31.00 ©2022 IEEE
Authorized licensed use limited to: Kansas State University. Downloaded on June 26,2023 at 13:46:48 UTC from IEEE Xplore. Restrictions apply.